Electromechanical Properties of Perfusion/Metabolism Mismatch: Comparison of Nonfluoroscopic Electroanatomic Mapping with ^{18}F-FDG PET

Senta Graf, MD[1]; Mariann Gyöngyösi, MD, PhD[1]; Aliasghar Khorsand, PhD[1]; Stephan G. Nekolla, PhD[2]; Christian Pirich, MD[3]; Kurt Kletter, MD[3]; Robert Dudczak, MD[3]; Dietmar Glogar, MD[1]; Gerold Porenta, MD, PhD[1]; and Heinz Sochor, MD[1]

[1]Department of Cardiology, Medical University of Vienna, Vienna, Austria; [2]Technische Universität München, Munich, Germany; and [3]Department of Nuclear Medicine, Medical University of Vienna, Vienna, Austria

The aim of this study was to compare nonfluoroscopic electroanatomic mapping (NOGA), SPECT perfusion imaging, and PET metabolic imaging for assessment of myocardial viability. In particular, we sought to elucidate differences of electromechanical properties between the perfusion/metabolism mismatch as an indicator of a potentially reversible ischemic injury and the perfusion/metabolism match indicating irreversibly damaged myocardial tissue. **Methods:** Twenty-one patients with coronary artery disease underwent NOGA mapping of endocardial unipolar voltage, cardiac ^{18}F-FDG PET of glucose utilization, and resting ^{201}Tl SPECT of myocardial perfusion. **Results:** Electrical activity was 10.8 ± 4.6 mV (mean ± SD) in normal myocardium and was unchanged in hypoperfused segments with maintained glucose metabolism (perfusion/metabolism mismatch), 9.3 ± 3.4 mV (P = not significant). In contrast, hypoperfused segments with a perfusion/metabolism match and nonviable segments showed significantly lower voltage (6.9 ± 3.1 mV, $P < 0.0001$ and 4.1 ± 1.1 mV, $P < 0.0001$ vs. normal). In hypoperfused segments, metabolic activity was more closely related to endocardial voltage than was myocardial perfusion (^{201}Tl vs. voltage: $r = 0.38$, SEE = 3.2, $P < 0.001$; ^{18}F-FDG PET vs. voltage: $r = 0.6$, SEE = 2.8, $P < 0.0001$). **Conclusion:** In hypoperfused myocardium, electrical activity by NOGA mapping is more closely related to PET metabolic activity than to SPECT myocardial perfusion. As NOGA mapping does not differentiate hypoperfused myocardium with enhanced glucose utilization from normal myocardium, results from NOGA mapping need to be correlated with results from perfusion imaging to identify hypoperfused, yet viable, myocardium and to stratify patients for revascularization procedures.

Key Words: myocardial metabolism; myocardial perfusion; nonfluoroscopic electroanatomic mapping; PET; coronary artery disease

J Nucl Med 2004; 45:1611–1618

Received Nov. 6, 2003; revision accepted Apr. 12, 2004.

For correspondence or reprints contact: Senta Graf, MD, Department of Cardiology, Medical University of Vienna, Waehringer Guertel 18-20, A-1090 Vienna, Austria.

E-mail: senta.graf@akh-wien.ac.at

Contractile dysfunction due to ischemic events has been shown to be potentially reversible when viability is maintained, such as in hibernating or stunned myocardium (*1–4*). Thus, the therapeutic stratification of patients with significant left ventricular (LV) dysfunction is strongly influenced by the detection of viable myocardium (*5*). By predicting the capacity of improvement of LV function after revascularization, viability assessment yields important additional prognostic information and aids in the clinical management of patients with ischemic heart disease (*6–8*).

Besides standard techniques such as conventional SPECT scintigraphy with ^{201}Tl or ^{99m}Tc-labeled tracers and low-dose dobutamine stress echocardiography for viability imaging, cardiac ^{18}F-FDG PET has been used for the assessment of myocardial tissue injury (*9,10*). The presence of maintained glucose metabolism in hypoperfused myocardium (perfusion/metabolism mismatch) has been demonstrated to accurately predict the recovery of contractile function and an improvement in the clinical course of the patient (*6–8*).

Recently, novel methods—such as transmyocardial revascularization approaches with the possibility of injection of growth factors, stem cells, plasmids encoding growth factors, or myoblasts—have become available that may offer treatment options to patients with severe ischemic heart disease who have no alternative of percutaneous or surgical revascularization. These new techniques are performed in the catheterization laboratory and therefore require the capability for an online detection of ischemically injured, yet viable, myocardial areas.

Nonfluoroscopic catheter-based electroanatomic mapping (NOGA) enables identification and localization of viable myocardial tissue by simultaneous assessment of electrical activation and local mechanical response of the heart in the catheterization laboratory (*11,12*). The overall diagnostic

value of endocardial mapping has been previously compared with SPECT (*13–15*), PET (*16–19*), and MRI (*20*). However, the specific electromechanical pattern of the perfusion/metabolism mismatch—characterized by decreased myocardial perfusion but enhanced ^{18}F-FDG uptake due to increased glucose metabolism in ischemic territories—has not been elucidated in detail.

Therefore, the aim of this study was to compare NOGA mapping with PET metabolic imaging and SPECT perfusion imaging. Polar map analysis was used to compare electromechanical properties of hypoperfused segments with maintained PET metabolic activity (perfusion/metabolism mismatch), as an indicator of a potentially reversible ischemic injury, with hypoperfused segments with reduced PET metabolic activity (perfusion/metabolism match) indicating irreversibly damaged myocardial tissue.

MATERIALS AND METHODS

Study Population

Twenty-one consecutive patients (16 men, 5 women; mean age ± SD, 61 ± 11 y) with angiographically proven significant coronary artery disease and stable angina pectoris were included in the study. Exclusion criteria were recent myocardial infarction (within 3 wk before the endocardial mapping and ^{18}F-FDG PET procedures), unstable angina, a LV ejection fraction < 30%, a LV wall thickness < 10 mm in any part of the left ventricle (to avoid an increased risk of perforating the thinned myocardium by an endocardial catheter), severe valvular heart disease, and severe peripheral atherosclerotic disease. Thirteen patients had experienced a previous myocardial infarction (3 ± 2 y before the study). Coronary angiography revealed multivessel disease in 13 patients. The LV ejection fraction measured by ventriculography (area length method) was 49% ± 17%.

Patients who were stratified to undergo NOGA mapping were studied by cardiac ^{18}F-FDG PET of glucose utilization and ^{201}Tl myocardial resting perfusion imaging 8 ± 2 and 4 ± 2 d, respectively, before NOGA mapping. All procedures were performed according to institutional guidelines. Informed consent was obtained from all patients.

^{201}Tl SPECT Perfusion Imaging

To evaluate myocardial perfusion, 100 MBq ^{201}Tl were injected intravenously under resting conditions. Ten minutes later, SPECT image acquisition was performed using a dual-detector γ-camera with a noncircular clockwise orbit (Vertex MCD; ADAC Laboratories). A total of 32 projections (16 per head) was obtained by step-and-shoot acquisition over 180°, performing a simultaneous transmission scan with ^{153}Gd to obtain attenuation-corrected images. Transaxial images were reconstructed using fully automated software for attenuation and scatter correction (Vantage, ADAC Laboratories; ExSPECT, Emory University).

^{18}F-FDG PET of Glucose Utilization

Patients were studied after fasting for at least 6 h. If fasting glucose levels were within the normal range, a 75-g oral glucose load was given to improve myocardial glucose uptake. Forty-five to 60 min later, the glucose level was determined, and 2–6 international units of insulin were injected intravenously if the glucose levels exceeded 140 mg/dL. This procedure was repeated until the glucose level was <140 mg/dL, at which time 400–500 MBq ^{18}F-FDG were injected. Thirty to 90 min after tracer injection, image acquisition was performed on a high-resolution, full-ring PET camera (Advance; General Electric). A 1-min scout scan for correct positioning of the heart was followed by a 10-min transmission scan for attenuation correction (using a ^{68}Ge source) and a 30-min static emission scan for myocardial ^{18}F-FDG uptake. Image reconstruction was performed to generate 35 transaxial images.

Analysis of SPECT and PET Images

Transaxial ^{201}Tl SPECT and ^{18}F-FDG PET images were transferred to an image-processing workstation (Onyx; SGI) for image analysis. For both SPECT and PET images, transaxial images were reoriented into short-axis and long-axis images, and a polar map analysis was performed (Munich Heart software) to derive segmental tracer uptake in 12 segments (4 anatomic regions: septal, anterior, lateral, and posterior; 3 short-axis planes: apical, midventricular, and basal) in accordance with the results available from the NOGA mapping system.

To define segments without perfusion abnormality as the segments with "normal" glucose uptake (*21*), average segmental ^{201}Tl and ^{18}F-FDG uptake values were normalized to the respective regions exhibiting the maximal ^{201}Tl uptake. Myocardial segments were classified into 4 groups according to viability criteria published in previous reports (*17,22–26*) differentiating viable myocardium (segments with normal perfusion or maintained glucose metabolism) from nonviable myocardium (hypoperfused segments with severely reduced glucose metabolism) as follows:

- Normal: Segments with ^{201}Tl uptake > 70% were considered as normally perfused.

All segments with reduced ^{201}Tl uptake (≤70%) were considered as hypoperfused and classified as:

- Perfusion/metabolism mismatch: hypoperfused myocardium with relatively increased glucose metabolism (^{201}Tl uptake ≤ 70%; ^{18}F-FDG uptake > 70%),
- Perfusion/metabolism match: hypoperfused myocardium with concordantly reduced glucose metabolism (^{201}Tl uptake ≤ 70%; ^{18}F-FDG uptake > 50% and ≤ 70%),
- Nonviable: hypoperfused myocardium without evidence of residual glucose metabolism (^{201}Tl uptake ≤ 70%; ^{18}F-FDG uptake ≤ 50%).

NOGA Mapping

After diagnostic coronary angiography and contrast ventriculography, electroanatomic mapping was performed. Under fluoroscopic guidance, a 7-French mapping catheter with a deflectable tip was advanced into the LV cavity. Electroanatomic mapping was performed as previously described (*11,27,28*) to measure endocardial unipolar voltage (UpV) and local linear shortening (LLS). Polar map analysis was used to generate segmental values of the LV endocardial voltage and LLS in 12 myocardial segments indicated earlier. Thus, a direct segmental comparison of the maps for endocardial voltage and LLS with myocardial perfusion and glucose utilization was achieved (Figs. 1 and 2).

During NOGA mapping an average of 95 ± 28 endocardial points per patient was investigated. After filtering endocardial

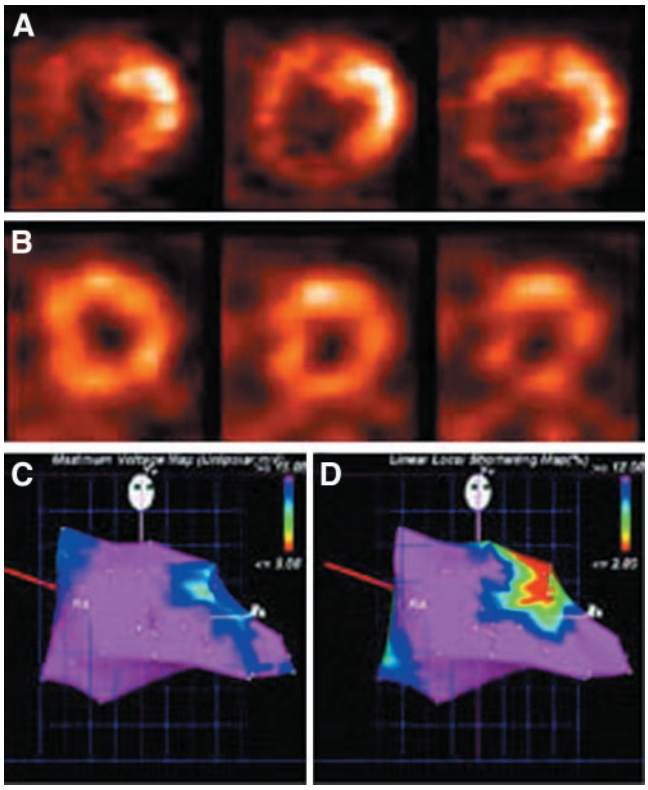

FIGURE 1. Short-axis views of ^{18}F-FDG PET (A) and ^{201}Tl SPECT scintigraphy (B) of 50-y-old patient with significant stenosis of circumflex artery with moderately decreased global LV function. Perfusion/metabolism mismatch is present in midlateral wall with reduced ^{201}Tl uptake and increased ^{18}F-FDG uptake. Electrical activity (unipolar voltage) was nearly normal in all segments (C), whereas LLS showed decreased values in midlateral wall (D).

points with inadequate voltage signals due to unstable location of the catheter or due to rhythm disturbances, the average number of points drawing the LV silhouette was 78 ± 22. Since the septal and posterolateral basal segments in the polar map analysis of the endocardial mapping in most cases exhibit low voltage values of the mitral valve apparatus and the base of the heart (*12*), these basal segments (n = 63) were excluded from further analysis. In 17 segments, no definite interpretation could be made because of too few (<3) sampled data points. Thus, 172 (68%) of the 252 myocardial segments were available for data analysis.

Statistics

The mean ± SD is given for continuous data. Categoric variables are described as frequency distribution. ANOVA was used for data comparison between groups; regression analysis was used to compare continuous data. Receiver-operating-characteristic (ROC) analysis was used to derive the optimal threshold level (highest diagnostic accuracy) for UpV to differentiate PET viable myocardium and PET nonviable myocardium. P values < 0.05 indicated statistical significance. Statistical analyses were performed with the Statview software package (Statview 5.0.1; SAS Institute) and the CLABROC and LABROC computer software (*29*).

RESULTS

Endocardial Voltage

Endocardial voltage was 10.8 ± 4.6 mV in normal segments (n = 88), 9.3 ± 3.4 mV in hypoperfused segments with a perfusion/metabolism mismatch (n = 29), 6.9 ± 3.1 mV in hypoperfused segments with a perfusion/metabolism match (n = 40), and 4.1 ± 1.1 mV in nonviable segments (n = 15). Endocardial voltage was not significantly different between normal segments and hypoperfused segments with a perfusion/metabolism mismatch (P = not significant [NS]) but was significantly lower in hypoperfused segments with a perfusion/metabolism match and in nonviable segments (P < 0.0001; Table 1).

Relation Between Myocardial Perfusion, Glucose Metabolism, and Endocardial Voltage

Correlation between myocardial perfusion and endocardial voltage was moderate for all myocardial segments (r = 0.41, r^2 = 0.17, SEE = 4.1, P < 0.0001; Fig. 3A) and decreased slightly when only hypoperfused segments were included in the analysis (r = 0.38, r^2 = 0.14, SEE = 3.2, P < 0.001; Fig. 3C). There was no significant correlation between myocardial perfusion and endocardial voltage in hypoperfused segments with a perfusion/metabolism mismatch (r = 0.2, r^2 = 0.04, SEE = 3.4, P = NS; Fig. 3E).

In contrast, correlation between glucose metabolism and endocardial voltage was moderate when all myocardial segments were included in the analysis (r = 0.45, r^2 = 0.20,

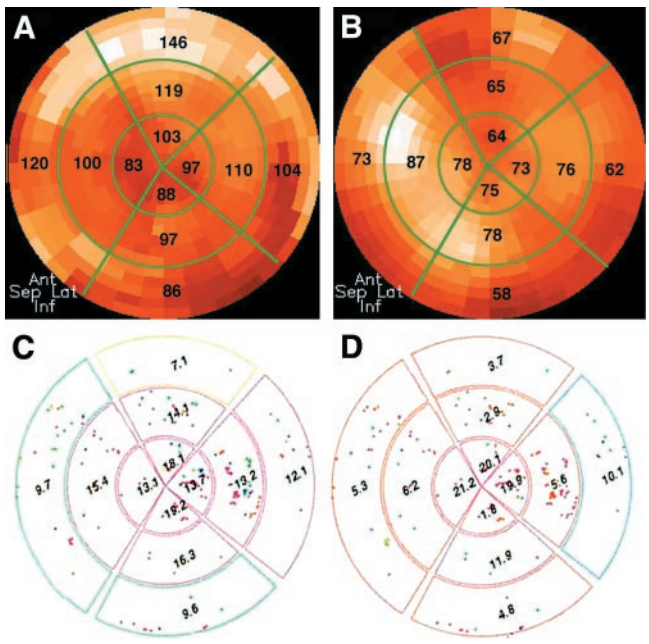

FIGURE 2. Polar map analysis of ^{18}F-FDG PET metabolic imaging (A) and ^{201}Tl perfusion imaging (B) and NOGA mapping (C, unipolar voltage; D, LLS) of patient with severe stenosis of diagonal branch of left anterior descending artery with perfusion/metabolism mismatch in basal and middle anterior and anterolateral walls with unipolar voltage values within normal range and reduced LLS values.

TABLE 1
Mean Endocardial Voltage (UpV), LLS, Normalized ^{18}F-FDG Uptake, and Normalized ^{201}Tl Uptake in Normal Myocardium, in Hypoperfused Myocardium with Maintained Glucose Metabolism (Mismatch), in Hypoperfused Myocardium with Concordantly Reduced Glucose Metabolism (Match), and in Hypoperfused Myocardium with Nonviable Tissue

Myocardium	*n*	UpV (mV)	LLS (%)	Normalized uptake (%)	
				^{18}F-FDG	^{201}Tl
Normal	88	10.8 ± 4.6	9.5 ± 7.1	95.5 ± 15.1	79.2 ± 5.8
Mismatch	29	9.3 ± 3.4	9.6 ± 7.2	92.3 ± 12.1	61.1 ± 7.5*
Match	40	6.9 ± 3.1†‡	9.4 ± 8.3	64.9 ± 8.5†‡	57.1 ± 10.6‡
Nonviable	15	4.1 ± 1.1§¶	5.4 ± 5.0‖	42.8 ± 4.8§¶	46.0 ± 14.7§¶

*$P < 0.0001$ mismatch vs. normal.
†$P < 0.001$ match vs. mismatch.
‡$P < 0.0001$ match vs. normal.
§$P < 0.05$ nonviable vs. match.
¶$P < 0.0001$ nonviable vs. mismatch or normal.
‖$P < 0.05$ nonviable vs. normal.

SEE = 4.0, $P < 0.0001$; Fig. 3B) and increased when only hypoperfused segments were considered ($r = 0.6$, $r^2 = 0.36$, SEE = 2.8, $P < 0.0001$; Fig. 3D). In hypoperfused segments with a perfusion/metabolism mismatch, glucose metabolism was significantly related to endocardial voltage ($r = 0.45$, $r^2 = 0.21$, SEE = 3.1, $P < 0.05$; Fig. 3F).

LLS

LLS was 9.5% ± 7.1% in normal segments, 9.6% ± 7.2% in hypoperfused segments with a perfusion/metabolism mismatch, 9.4% ± 8.3% in hypoperfused segments with a perfusion/metabolism match, and 5.4% ± 5.0% in nonviable segments. There was no significant difference

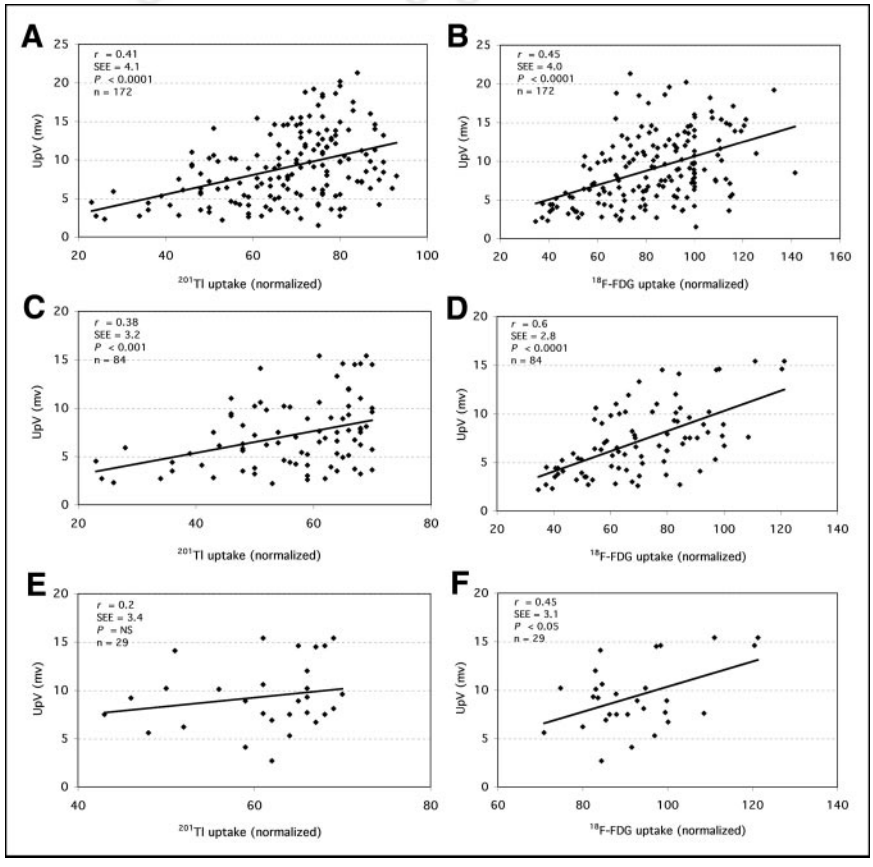

FIGURE 3. Linear correlation between UpV by NOGA mapping and normalized ^{201}Tl and ^{18}F-FDG uptake in all myocardial segments (A, ^{201}Tl: $P < 0.0001$, $r = 0.41$, $r^2 = 0.17$, SEE = 4.1; B, ^{18}F-FDG: $P < 0.0001$, $r = 0.45$, $r^2 = 0.20$, SEE = 4.0), in hypoperfused segments (C, ^{201}Tl: $P < 0.001$, $r = 0.38$, $r^2 = 0.14$, SEE = 3.2; D, ^{18}F-FDG: $P < 0.0001$, $r = 0.6$, $r^2 = 0.36$, SEE = 2.8), and in segments with perfusion/metabolism mismatch (E, ^{201}Tl: P = NS, $r = 0.2$, $r^2 = 0.04$, SEE = 3.4; F, ^{18}F-FDG: $P < 0.05$, $r = 0.45$, $r^2 = 0.21$, SEE = 3.1).

between normal segments, hypoperfused segments with a perfusion/metabolism mismatch, and hypoperfused segments with a perfusion/metabolism match (Table 1).

ROC Analysis

The threshold level for endocardial voltage to identify PET viable segments with the highest achievable accuracy by ROC analysis was 5.2 mV. This threshold level was associated with a sensitivity and specificity of 85% for the detection of PET viable tissue by the mapping of endocardial voltage (Fig. 4A). ROC analysis of endocardial voltage and LLS to differentiate between PET viable segments (^{18}F-FDG uptake $>$ 50%) and PET nonviable segments (^{18}F-FDG uptake $\leq$ 50%) showed an area under the ROC curve of 0.9 $\pm$ 0.03 and 0.69 $\pm$ 0.06, respectively (Fig. 4B).

For the 4 anatomic regions, ROC analysis of endocardial voltage revealed an area under the curve of 0.91 $\pm$ 0.06 for the septal region, 0.91 $\pm$ 0.04 for the anterior region, 0.83 $\pm$ 0.07 for the lateral region, and 0.87 $\pm$ 0.09 for the inferior region.

DISCUSSION

This study investigated the relation between the electrical properties of myocardial tissue and imaging of myocardial perfusion and glucose metabolism for viability assessment. The impact of perfusion/metabolism imaging for the prediction of major adverse cardiac events (death and myocardial infarction) and the improvement of LV function after revascularization has previously been well described (*6–8,30,31*). The new catheter technique of electromechanical NOGA mapping has previously been compared with different scintigraphic methods (*13–19*) (Table 2). However, to our knowledge, the electromechanical properties of hypoperfused myocardial segments with a perfusion/metabolism mismatch as the hallmark for reversibly injured tissue have not been investigated in detail.

Endocardial Voltage

Measurements of voltage obtained in normal myocardium (10.8 $\pm$ 4.6 mV) and in scarred segments (4.1 $\pm$ 1.1 mV) in this study are in good agreement with results of previous studies, which demonstrated that NOGA mapping can be used to identify viable myocardium (*13–20*) (Table 2).

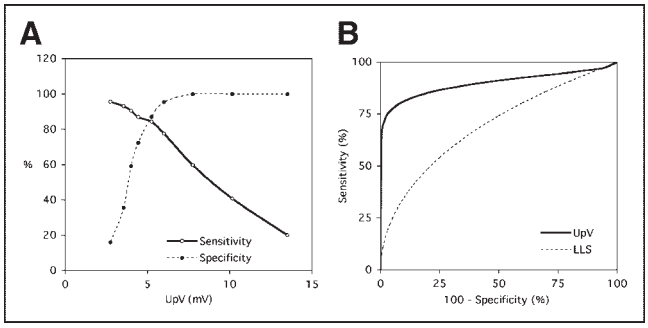

FIGURE 4. (A) Determination of threshold value of unipolar endocardial voltage for identification of PET viable myocardium with sensitivity and specificity of 85% based on threshold of 5.2 mV. (B) ROC curves of UpV and LLS for differentiation between PET viable and PET nonviable myocardium with area under the curve of 0.9 $\pm$ 0.03 and 0.69 $\pm$ 0.06, respectively.

Hypoperfused myocardial segments that exhibit a maintained glucose metabolism in the absence of adequate oxygen supply showed values for endocardial voltage that were similar to values derived in segments with a normal perfusion. This finding suggests that "electrical viability" is closely related to the metabolic state of the myocardial cell and can be retained even when perfusion is reduced.

A moderate correlation was found between myocardial ^{18}F-FDG uptake and endocardial voltage (r = 0.45) when all segments were included in the analysis. The exclusion of myocardial segments with normal perfusion resulted in an improved correlation between ^{18}F-FDG uptake and endocardial voltage (r = 0.6). In contrast, the correlation between endocardial voltage and myocardial perfusion decreased when only hypoperfused segments were investigated and became insignificant when only hypoperfused segments with a perfusion/metabolism mismatch were included. These findings support the concept of a close concordance between maintained or increased myocardial glucose metabolism and electrical activity in hypoperfused myocardium.

The present study confirms that resting perfusion imaging by ^{201}Tl is unable to differentiate hypoperfused segments with enhanced or preserved metabolism and preserved electrical activity from hypoperfused segments with a concordant reduction in metabolism and electrical activity.

In this study, the sensitivity and specificity of endocardial voltage for assessment of viability were 85% and, thus, comparable to data obtained by other techniques. The threshold value of endocardial voltage to differentiate viable and nonviable myocardium obtained by ROC analysis in this study was 5.2 mV and differed slightly from our previously published threshold value of 6.4 mV, which was obtained on the basis of ^{201}Tl late resting uptake (*13*). This lower threshold may partly be attributed to a lower accuracy of viability detection by ^{201}Tl and to differences in the study population.

LLS

Measurements of LLS were similar between normal segments, segments with a perfusion/metabolism mismatch, and segments with a perfusion/metabolism match. Accordingly, LLS cannot differentiate between normal and hypoperfused myocardium with maintained viability, as demonstrated by ROC analysis. The sensitivity and specificity of LLS for detection of viable and nonviable tissues were low, as demonstrated in previous studies (*13,14,16,19*) (Table 2). Therefore, our study confirms the limited value of LLS for the assessment of myocardial viability.

Limitations

This study included patients with an ejection fraction $>$ 30%, as initially NOGA mapping with a 7-French catheter

TABLE 2
Comparison of Electromechanical NOGA Mapping with Different Myocardial Imaging Methods

Reference	No. of patients	Reference methods	EF method	EF baseline/ EF follow-up	Sens (%)	Spec (%)	UpV threshold (mV)	Comments
Kornowski et al. (*15*)	18	^{201}Tl rest, ^{99m}Tc stress	—	—	—	—	—	UpV and LLS highest in normal segments, mild reduction in reversible segments, lowest in scar
Fuchs et al. (*14*)	61	^{201}Tl rest, ^{99m}Tc stress		48 ± 11 —	90	90	5.4	Stress-induced ischemia: UpV threshold, 9.0 mV; Sens, 68%; Spec, 67%; LLS less sensitive and specific than UpV
Gyöngyösi et al. (*13*)	32	^{201}Tl	Catheter	40 ± 8 —	82	82	6.4	Only weak correlation between ^{201}Tl and LLS
Botker et al. (*16*)	31	^{13}N-NH_3, ^{18}F-FDG, 3D Echo	Echo	30 ± 9 —	69	69	6.5	LLS: no difference between normal and dysfunctional myocardium
Koch et al. (*17*)	46	^{18}F-FDG, ^{99m}Tc	Catheter	52 ± 16 62 ± 13	77	75	7.5	Regional wall motion increased in "infarct" areas when UpV > 7.5 mV; no additional information from LLS
Keck et al. (*18*)	51	^{18}F-FDG, ^{99m}Tc rest and stress	Echo	51 ± 14 —	65	90	4.5	Stress perfusion: UpV in reversible segments not different from normal. LLS cannot predict recovery but differentiates between normal, hypokinetic myocardium and scar tissue
Wiggers et al. (*19*)	20	^{18}F-FDG, ^{99m}Tc	Echo or MRI	29 ± 6 34 ± 13	59*	59*	8.4*	Recovery of LV function more predictable by PET or SPECT than by UpV in dysfunctional myocardium. LLS: no difference in reversibly and irreversibly dysfunctional regions
Perin et al. (*20*)	15	MRI	—	—	93	88	6.9	Subendocardial scar: UpV threshold, 7.9 mV; Sens, 88%; Spec, 88%
This study	21	^{18}F-FDG, ^{201}Tl	Catheter	49 ± 17 —	85	85	5.2	UpV in hypoperfused myocardium is more closely related to ^{18}F-FDG PET than to SPECT myocardial perfusion, especially in perfusion/metabolism mismatch

*Distinction between reversible and irreversible dysfunction; all other values for sensitivity and specificity distinction are between viable myocardium and scar tissue.

EF = LV ejection fraction (%); Sens = sensitivity; Spec = specificity; ^{99m}Tc = ^{99m}Tc-sestamibi; Catheter = center-line method from digitized angiograms; Echo = echocardiography; 3D = 3-dimensional.

was considered to carry an increased risk of myocardial perforation in myocardium with a thinned wall. Therefore, whether the results also would apply to patients with a severely reduced LV function (<30% ejection fraction) remains to be determined.

Different criteria to define myocardial viability by ^{201}Tl or ^{18}F-FDG imaging have been proposed in previous studies (*6*,*22*,*23*,*25*,*32*,*33*). In agreement with the study of Koch et al. (*17*), who compared NOGA mapping with SPECT and PET, in the present study a normalized ^{201}Tl tracer uptake > 70% was used for definition of normal perfusion and a normalized ^{18}F-FDG tracer uptake ≤ 50% was used for definition of nonviable myocardium. Unlike an earlier study that used late ^{201}Tl imaging to delineate myocardial viability (*13*), resting ^{201}Tl SPECT in the present study was performed immediately after tracer injection to delineate resting myocardial perfusion.

The commercial software for NOGA analysis generates data displays in a polar map format. Therefore, segmental polar map analysis was used to achieve a direct semiquantitative comparison of results from NOGA mapping and scintigraphic imaging. However, differences may have occurred, as the 2 methods use different principles of signal processing: NOGA is based on a discrete point-per-point registration of values by a catheter, whereas scintigraphic images obtained by a tomographic acquisition represent a continuous imaging map. Moreover, small misalignments between SPECT and PET data cannot be excluded, as both studies were performed on different days and with different cameras. However, because all scintigraphic studies were processed with the same image analysis software, significant errors due to misalignment of segments are unlikely.

In NOGA mapping, the basal portion of the septal and posterolateral segments of the left ventricle are difficult to evaluate. Moreover, nondiagnostic endocardial signals due to an unstable location of the catheter or due to arrhythmias had to be excluded from analysis. Thus, NOGA mapping frequently does not cover the entire endocardial surface. Furthermore, segments with a perfusion/metabolism mismatch are not common in clinical practice, as reflected by the low number of 29 mismatch segments (17% of all measurable segments). Also, small areas of a perfusion/metabolism mismatch can be missed by segmental polar map analysis, particularly when overlapping between segments occurs.

Finally, even though the accuracy of PET viability imaging to predict functional recovery is well established (*8*,*34*), functional recovery as an endpoint of viability was not investigated independently in the present study.

CONCLUSION

In hypoperfused myocardium, endocardial electrical activity by NOGA mapping is more closely related to PET metabolic activity than to SPECT myocardial perfusion. Hypoperfused myocardial segments with a perfusion/metabolism mismatch as a hallmark of maintained myocardial viability exhibit maintained endocardial potential similar to segments with a normal perfusion. Thus, although NOGA mapping correlates with maintained metabolic activity, an assessment of myocardial perfusion needs to be made if NOGA mapping is to be used to differentiate normal myocardium from hypoperfused myocardium with preserved viability and to guide online decision making for endocavitary or intraluminal revascularization procedures. Moreover, a complementary imaging technique for assessment of myocardial viability may be needed, as NOGA mapping rarely covers the entire endocardial surface.

ACKNOWLEDGMENTS

We are grateful for the support and superb technical assistance of the technicians in the laboratory for cardiovascular nuclear medicine as well as the nurses working in the coronary catheterization laboratory of the Department of Cardiology and the technologists of the PET center of the Department of Nuclear Medicine at the Medical University of Vienna Medical School. This work was supported in part by the Verein zur Förderung der Wissenschaftlichen Forschung am Rudolfinerhaus.

REFERENCES

1. Braunwald E, Kloner RA. The stunned myocardium: prolonged, postischemic ventricular dysfunction. *Circulation.* 1982;66:1146–1149.
2. Braunwald E, Rutherford JD. Reversible ischemic left ventricular dysfunction: evidence for the "hibernating myocardium." *J Am Coll Cardiol.* 1986;8:1467–1470.
3. Baer FM, Erdmann E. Methods of assessment and clinical relevance of myocardial hibernation and stunning: assessment of myocardial viability. *Thorac Cardiovasc Surg.* 1998;46(suppl 2):264–269.
4. Vanoverschelde JL, Wijns W, Depre C, et al. Mechanisms of chronic regional postischemic dysfunction in humans: new insights from the study of noninfarcted collateral-dependent myocardium. *Circulation.* 1993;87:1513–1523.
5. Beller GA. Selecting patients with ischemic cardiomyopathy for medical treatment, revascularization, or heart transplantation. *J Nucl Cardiol.* 1997;4:S152–S157.
6. Tillisch J, Brunken R, Marshall R, et al. Reversibility of cardiac wall-motion abnormalities predicted by positron tomography. *N Engl J Med.* 1986;314:884–888.
7. Eitzman D, al-Aouar Z, Kanter HL, et al. Clinical outcome of patients with advanced coronary artery disease after viability studies with positron emission tomography. *J Am Coll Cardiol.* 1992;20:559–565.
8. Di Carli MF, Davidson M, Little R, et al. Value of metabolic imaging with positron emission tomography for evaluating prognosis in patients with coronary artery disease and left ventricular dysfunction. *Am J Cardiol.* 1994;73:527–533.
9. Marshall RC, Tillisch JH, Phelps ME, et al. Identification and differentiation of resting myocardial ischemia and infarction in man with positron computed tomography, ^{18}F-labeled fluorodeoxyglucose and N-13 ammonia. *Circulation.* 1983;67:766–778.
10. Schelbert HR. ^{18}F-Deoxyglucose and the assessment of myocardial viability. *Semin Nucl Med.* 2002;32:60–69.
11. Gepstein L, Hayam G, Ben-Haim SA. A novel method for nonfluoroscopic catheter-based electroanatomical mapping of the heart: in vitro and in vivo accuracy results. *Circulation.* 1997;95:1611–1622.
12. Kornowski R, Hong MK, Gepstein L, et al. Preliminary animal and clinical experiences using an electromechanical endocardial mapping procedure to distinguish infarcted from healthy myocardium. *Circulation.* 1998;98:1116–1124.
13. Gyöngyösi M, Sochor H, Khorsand A, Gepstein L, Glogar D. Online myocardial viability assessment in the catheterization laboratory via NOGA electroanatomic mapping: quantitative comparison with thallium-201 uptake. *Circulation.* 2001;104:1005–1011.
14. Fuchs S, Hendel RC, Baim DS, et al. Comparison of endocardial electromechan-

ical mapping with radionuclide perfusion imaging to assess myocardial viability and severity of myocardial ischemia in angina pectoris. *Am J Cardiol.* 2001;87: 874–880.
15. Kornowski R, Hong MK, Leon MB. Comparison between left ventricular electromechanical mapping and radionuclide perfusion imaging for detection of myocardial viability. *Circulation.* 1998;98:1837–1841.
16. Botker HE, Lassen JF, Hermansen F, et al. Electromechanical mapping for detection of myocardial viability in patients with ischemic cardiomyopathy. *Circulation.* 2001;103:1631–1637.
17. Koch KC, vom Dahl J, Wenderdel M, et al. Myocardial viability assessment by endocardial electroanatomic mapping: comparison with metabolic imaging and functional recovery after coronary revascularization. *J Am Coll Cardiol.* 2001; 38:91–98.
18. Keck A, Hertting K, Schwartz Y, et al. Electromechanical mapping for determination of myocardial contractility and viability: a comparison with echocardiography, myocardial single-photon emission computed tomography, and positron emission tomography. *J Am Coll Cardiol.* 2002;40:1067–1074.
19. Wiggers H, Botker HE, Sogaard P, et al. Electroanatomical mapping versus positron emission tomography and single photon emission computed tomography for the detection of myocardial viability in patients with ischemic cardiomyopathy. *J Am Coll Cardiol.* 2003;41:843–848.
20. Perin EC, Silva GV, Sarmento-Leite R, et al. Assessing myocardial viability and infarct transmurality with left ventricular electromechanical mapping in patients with stable coronary artery disease: validation by delayed-enhancement magnetic resonance imaging. *Circulation.* 2002;106:957–961.
21. Camici P, Ferrannini E, Opie LH. Myocardial metabolism in ischemic heart disease: basic principles and application to imaging by positron emission tomography. *Prog Cardiovasc Dis.* 1989;32:217–238.
22. Burt RW, Perkins OW, Oppenheim BE, et al. Direct comparison of fluorine-18-FDG SPECT, fluorine-18-FDG PET and rest thallium-201 SPECT for detection of myocardial viability. *J Nucl Med.* 1995;36:176–179.
23. Altehoefer C, vom Dahl J, Buell U, Uebis R, Kleinhans E, Hanrath P. Comparison of thallium-201 single-photon emission tomography after rest injection and fluorodeoxyglucose positron emission tomography for assessment of myocardial viability in patients with chronic coronary artery disease. *Eur J Nucl Med.* 1994;21:37–45.
24. Srinivasan G, Kitsiou AN, Bacharach SL, Bartlett ML, Miller-Davis C, Dilsizian V. [^{18}F]Fluorodeoxyglucose single photon emission computed tomography: can it replace PET and thallium SPECT for the assessment of myocardial viability? *Circulation.* 1998;97:843–850.
25. vom Dahl J, Altehoefer C, Sheehan FH, et al. Effect of myocardial viability assessed by technetium-99m-sestamibi SPECT and fluorine-18-FDG PET on clinical outcome in coronary artery disease. *J Nucl Med.* 1997;38:742–748.
26. Huitink JM, Visser FC, Bax JJ, et al. Predictive value of planar ^{18}F-fluorodeoxyglucose imaging for cardiac events in patients after acute myocardial infarction. *Am J Cardiol.* 1998;81:1072–1077.
27. Ben-Haim SA, Osadchy D, Schuster I, Gepstein L, Hayam G, Josephson ME. Nonfluoroscopic, in vivo navigation and mapping technology. *Nat Med.* 1996;2: 1393–1395.
28. Gepstein L, Hayam G, Shpun S, Ben-Haim SA. Hemodynamic evaluation of the heart with a nonfluoroscopic electromechanical mapping technique. *Circulation.* 1997;96:3672–3680.
29. Metz CE, Herman BA, Roe CA. Statistical comparison of two ROC-curve estimates obtained from partially-paired datasets. *Med Decis Making.* 1998;18: 110–121.
30. Di Carli MF, Asgarzadie F, Schelbert HR, et al. Quantitative relation between myocardial viability and improvement in heart failure symptoms after revascularization in patients with ischemic cardiomyopathy. *Circulation.* 1995;92:3436–3444.
31. Zhang X, Liu XJ, Wu Q, et al. Clinical outcome of patients with previous myocardial infarction and left ventricular dysfunction assessed with myocardial ^{99m}Tc-MIBI SPECT and ^{18}F-FDG PET. *J Nucl Med.* 2001;42:166–173.
32. Bonow RO, Dilsizian V, Cuocolo A, Bacharach SL. Identification of viable myocardium in patients with chronic coronary artery disease and left ventricular dysfunction: comparison of thallium scintigraphy with reinjection and PET imaging with ^{18}F-fluorodeoxyglucose. *Circulation.* 1991;83:26–37.
33. Marwick TH, MacIntyre WJ, Lafont A, Nemec JJ, Salcedo EE. Metabolic responses of hibernating and infarcted myocardium to revascularization: a follow-up study of regional perfusion, function, and metabolism. *Circulation.* 1992; 85:1347–1353.
34. Bax JJ, Visser FC, Poldermans D, et al. Relationship between preoperative viability and postoperative improvement in LVEF and heart failure symptoms. *J Nucl Med.* 2001;42:79–86.

The Journal of NUCLEAR MEDICINE

Electromechanical Properties of Perfusion/Metabolism Mismatch: Comparison of Nonfluoroscopic Electroanatomic Mapping with ^{18}F-FDG PET

Senta Graf, Mariann Gyöngyösi, Aliasghar Khorsand, Stephan G. Nekolla, Christian Pirich, Kurt Kletter, Robert Dudczak, Dietmar Glogar, Gerold Porenta and Heinz Sochor

J Nucl Med. 2004;45:1611-1618.

The Journal of Nuclear Medicine is published monthly.
SNMMI | Society of Nuclear Medicine and Molecular Imaging
1850 Samuel Morse Drive, Reston, VA 20190.
(Print ISSN: 0161-5505, Online ISSN: 2159-662X)

SNMMI SOCIETY OF NUCLEAR MEDICINE AND MOLECULAR IMAGING